

ORIGINAL ARTICLE

Development of a novel lactate dehydrogenase A inhibitor with potent antitumor activity and immune activation

Mengyan Du^{1,2,3} | Ting Yu⁴ | Qinjing Zhan⁵ | Han Li⁶ | Yiping Zou⁵ |
Meiyu Geng^{1,2,3} | Tao Meng⁴ | Zuoquan Xie^{1,3} 

¹State Key Laboratory of Drug Research, Shanghai Institute of Materia Medica, Chinese Academy of Sciences, Shanghai, China

²School of Life Science and Technology ShanghaiTech University, Shanghai, China

³University of Chinese Academy of Sciences, Beijing, China

⁴Division of Medicinal Chemistry, Shanghai Institute of Materia Medica, Chinese Academy of Sciences, Shanghai, China

⁵Jiangxi Key Laboratory of Active Ingredients of Natural Drugs, Yichun University, Yichun, China

⁶College of Pharmacy Nanjing University of Chinese Medicine, Nanjing, China

Correspondence

Tao Meng and Zuoquan Xie, Shanghai Institute of Materia Medica, 555 Zuchongzhi Road, Shanghai 201203, China.
Emails: tmeng@simm.ac.cn (T.M.); zqxie@simm.ac.cn (Z.X.)

Funding information

National Natural Science Foundation of China for Innovation Research Group, Grant/Award Number: 81821005; Shanghai Pujiang Program, Grant/Award Number: 18PJD052; Collaborative Innovation Cluster Project of Shanghai Municipal Commission of Health and Family Planning, Grant/Award Number: 2020CXJQ02

Abstract

Lactate accumulation in the tumor microenvironment was shown to be closely related to tumor growth and immune escape, and suppression of lactate production by inhibiting lactate dehydrogenase A (LDHA) has been pursued as a potential novel antitumor strategy. However, only a few potent LDHA inhibitors have been developed and most of them did not show potent antitumor effects in vivo. To this end, we designed new LDHA inhibitors and obtained a novel potent LDHA inhibitor, ML-05. ML-05 inhibited cellular lactate production and tumor cell proliferation, which was associated with inhibition of ATP production and induction of reactive oxygen species and G₁ phase arrest. In a mouse B16F10 melanoma model, intratumoral injection of ML-05 significantly reduced lactate production, inhibited tumor growth, and released antitumor immune response of T cell subsets (Th1 and GMZB⁺CD8 T cells) in the tumor microenvironment. Moreover, ML-05 treatment combined with programmed cell death-1 Ab or stimulator of interferon genes protein (STING) could sensitize the antitumor activity in B16F10 melanoma model. Collectively, we developed a novel potent LDHA inhibitor, ML-05, that elicited profound antitumor activity when injected locally, and was associated with the activation of antitumor immunity. In addition, ML-05 could sensitize immunotherapies, which suggests great translational value.

KEYWORDS

immunity, lactate, LDHA inhibitor, metabolic reprogramming, tumor microenvironment

Abbreviations: APC, allophycocyanin; diABZI, diamidobenzimidazole; ECAR, extracellular acidification rate; GMZB, granzyme B; IFN- γ , interferon- γ ; i.t., intratumorally; LDHA, lactate dehydrogenase A; PD-1, programmed cell death-1; PE, phycoerythrin; P/S, penicillin/streptomycin; Rb, retinoblastoma; ROS, reactive oxygen species; STING, stimulator of interferon genes; TGI, tumor growth inhibition; Th, T helper cell; TME, tumor microenvironment; Treg, regulatory T cell.

Mengyan Du and Ting Yu contributed equally to this work.

This is an open access article under the terms of the [Creative Commons Attribution-NonCommercial](https://creativecommons.org/licenses/by-nc/4.0/) License, which permits use, distribution and reproduction in any medium, provided the original work is properly cited and is not used for commercial purposes.

© 2022 The Authors. *Cancer Science* published by John Wiley & Sons Australia, Ltd on behalf of Japanese Cancer Association.

1 | INTRODUCTION

Metabolic reprogramming of tumors creates spatial and temporal heterogeneity in the TME, which profoundly affects the infiltration and phenotype of immune cells during tumor progression.^{1,2} Among the different types of metabolic remodeling, the first recognized feature of metabolic reprogramming is aerobic glycolysis in cancer. Tumor cells prefer to use glycolysis and generate large amounts of lactate, which is secreted outside of cells even under adequate oxygen supply, well-known as the Warburg effect.³ Lactate is the product of glycolysis, which promotes cell proliferation and neovascularization.⁴ Importantly, high levels of lactate lead to acidosis of the TME and induce immunosuppression through multiple mechanisms, including the inhibition of monocyte differentiation to dendritic cells and dendritic cell activation,⁵ recruitment of myeloid-derived suppressor cell-like immunosuppressive cell infiltration,^{6,7} and the inhibition of T cells and natural killer cells.^{8,9} Therefore, inhibition of lactate production in the TME has been pursued as a novel antitumor strategy or as an adjuvant for immunotherapy.

Lactate dehydrogenase A catalyzes the production of lactate in glycolysis,¹⁰ which is overexpressed in most types of cancers,^{11,12} and its depletion led to the inhibition of tumor growth in multiple tumor models.¹³⁻¹⁵ Moreover, the absence of LDHA in bone marrow cells triggers antitumor immunity, and increased glycolysis in tumor are characteristics of immune system resistance to adaptive T cell therapies,^{16,17} suggesting the important impact of LDHA on the TME and immunotherapy. Therefore, inhibition of LDHA activity in tumors could improve the immune microenvironment and initiate antitumor immunity.

To date, several LDHA inhibitors have been developed. Oxamate is a pyruvate analogue that was developed as the first LDHA inhibitor; however, it has a very low effect on LDHA activity with IC_{50} of approximately 800 μ M.¹⁸ Since 2010, compounds such as FX-11¹⁹ (Figure 1), *N*-hydroxyindole-2-carboxylates,²⁰ dicarboxylic acids,²¹ 2-thio-6-oxo-1,6-dihydropyrimidines,²² 2-amino-5-aryl-pyrazines,²³ and 3-hydroxy-2-mercaptocyclohex-2-enones²⁴ have been reported as LDHA inhibitors with IC_{50} at micromolar or submicromolar levels. Recently, more potent LDHA inhibitors have been developed with IC_{50} at nanomolar levels, such as quinoline 3-sulfonamides (GSK2837808A),²⁵ GNE-140,²⁶ and pyrazole-based compound 63²⁷

(Figure 1). However, most LDHA inhibitors did not show potent in vivo antitumor effects, which could relate to their inhibitory activity, metabolic stability, or route of administration. Furthermore, it remains unclear whether and how LDHA inhibitors improve the immunosuppressive TME to release antitumor immunity. To this end, in the current study we designed novel LDHA inhibitors and tested their antitumor activity both in vitro and in vivo, as well as their influence on the tumor immune microenvironment.

2 | MATERIALS AND METHODS

2.1 | Cell lines

A375, B16F10, EMT6, MIA PACA2, MDA-MB-468, HMCB, 4T-1, LLC, and PAN02 cells were obtained from ATCC. CAL51 cells were obtained from DSMZ. CAL51, LLC, and PAN02 cells were cultured in DMEM with 10% FBS and 1% P/S. MIA PACA2 cells were cultured in DMEM supplemented with 15% FBS and 2.5% horse serum and 1% P/S. A375 cells were cultured in DMEM with 10% FBS and 1% P/S. EMT6 cells were cultured in Waymouth MB752 with 15% FBS, 2 mL glutamine, and 1% P/S. All cells were cultured at 37°C in an incubator containing 5% CO₂.

2.2 | Lactate measurement

Tumor cells were plated into 96-well plates (1.5×10^4 /well) and then treated with serial doses of compound or 1% DMSO as a vehicle control in serum-free medium. After 6 h, the cell supernatants were measured by lactate assay according to the instruction kit (A019-2; Nanjing Jiancheng). The EC_{50} was calculated by GraphPad software as the concentration-inhibition rate concentration curve.

2.3 | Extracellular acidification rate assay

B16F10 cells (1×10^4 /well) were inoculated in XF96 cell culture plates (#09021) overnight. After 6 h of treatment, cells were incubated in assay solution containing 2 mmol/L glutamine in a CO₂-free

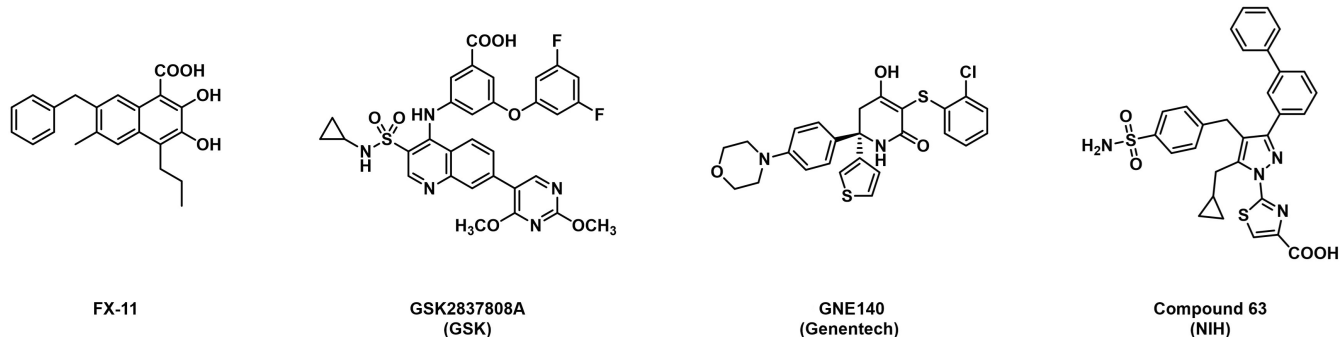


FIGURE 1 Structures of representative lactate dehydrogenase A inhibitors

incubator at 37°C for 1 h. Agilent Seahorse XF Glycolysis Stress Test Kit (#103020-100) was used to detect extracellular acidification rate. Prehydrated probe plates were replaced with XF Calibrant (pH 7.4, #100840-000) and incubated together with cell plates. After setting the program, the probe plates were placed in the instrument for 20 min to equilibrate, and then the cell plates were placed and assayed in the XF-96 analyzer (Seahorse Bioscience) using Wave software. The measurement of the extracellular acidification rate was expressed as mpH/min.

2.4 | Animal studies

Animal experiments were approved by the Animal Care and Use Committee of the Shanghai Institute of Materia Medica and carried out according to the Ethics Guidelines for Animal Care. C57BL/6 mice and nude mice were purchased from Beijing Viton Leve and held under specific pathogen-free conditions.

In a mouse melanoma model, B16F10 cells (1×10^5) were subcutaneously injected into 8-week-old C57BL/6 female mice or nude mice. When the tumor size reached approximately 100 mm^3 , mice were treated with vehicle (5% DMSO + 5% Kolliphor HS15 dissolved in saline), ML-05, or GNE140 at 50 mg/kg i.t., 100 mg/kg i.p., or 100 mg/kg orally once daily. For assessment of the tumor growth inhibitory effect of blockade of LDHA in vivo, B16F10 cells (1×10^5) were subcutaneously injected into C57BL/6 female mice (8 weeks old). 2'-OMe (50 μl) and 5'-Chol (cholesterol) modified siLDHA (5 nmol; RiboBio) or saline was injected directly into the tumor tissue at 3-day intervals.

For drug combination experiments (ML-05 and PD-1 Ab), B16F10 cells (1×10^5) were subcutaneously injected into C57BL/6 female mice (6–8 weeks). Mice were randomized to four treatment groups when the tumor size reached approximately 100 mm^3 : vehicle, PD-1 Ab, ML-05, and ML-05 plus PD-1 Ab. ML-05 (50 mg/kg i.t.) was injected daily and PD-1 Ab (BioXCell) at 200 μg i.p. per mouse every 3 days. For the ML-05 combined with diABZI experiment, similarly, mice were randomized into different treatment groups: vehicle, diABZI, ML-05, and ML-05 plus diABZI. ML-05 was injected daily (50 mg/kg i.t.) and diABZI (0.5 mg/kg i.p.) on days 1, 4, and 7.

Tumor volume $\left(\frac{\text{width}^2 \times \text{length}}{2} \right)$ was measured twice a week for all animal experiments. The mice were anesthetized and killed and the intact tumor tissue was removed for weighing.

2.5 | Flow cytometry analysis

B16F10 cells (1×10^5) were subcutaneously injected into C57BL/6 mice. Mice were treated with vehicle (5% DMSO + 5% Kolliphor HS15 dissolved in saline), ML-05, or GNE140 (50 mg/kg i.t.) daily for 7 days. Six hours after the last drug treatment, mouse tumor tissues were sheared to puree on ice and digested in solution containing 0.01% DNase I and 0.1% type IV collagenase (Sigma-Aldrich)

in RPMI-1640 serum-free medium at 37°C for 30 min. Tumor tissues were filtered through a 70 μm cell strainer (BD Biosciences) after termination of digestion with serum-bearing medium. After the lysis of erythrocytes at room temperature, the cell precipitate was resuspended for counting. For intracellular cytokine staining, 6×10^6 cells were inoculated in RPMI-1640 supplemented with 10% FCS and Leukocyte Activation Cocktail with GolgiPlug (550583; BD Pharmingen) for 5 h at 37°C. The cells were then washed with PBS and stained with Fixable Viability Stain 780 (565388; BD Pharmingen). Cells were then washed with MACS buffer (554656; BD Pharmingen) and stained with anti-CD45 BV510 (563891; BD Pharmingen), anti-CD3 APC (100236; BioLegend), anti-CD4 FITC (553046; BD Pharmingen), anti-CD45 FITC (103108; BioLegend), anti-CD8 BUV395 (563786; BD Pharmingen), anti-CD25 PE-CY7 (552880; BD Pharmingen), anti-CD11b BUV395 (563553; BD Pharmingen), anti-F4/80 BV421 (123132; BD Pharmingen), and anti-CD86 PE-CY7 (105014; BD Pharmingen). After washing twice with MACS buffer, cells were fixed for 50 min and permeabilized by Staining Buffer Set (421403; eBioscience) and stained intracellularly with anti-IFN- γ BUV737 (612769; BD Pharmingen), anti-granzyme BV421 (396414; BD Pharmingen), anti-IL-17A BV421 (563354; BD Pharmingen), anti-FOXP3 PE (560480; BD Pharmingen), anti-CD206 APC (141708; BD Pharmingen) for 50 min. Cells were fixed in paraformaldehyde for 10 min. Sorting was carried out on a BD LSRFortessa cell analyzer after cells were resuspended with MACS buffer. Data were analyzed with FlowJo software.

2.6 | Statistical analysis

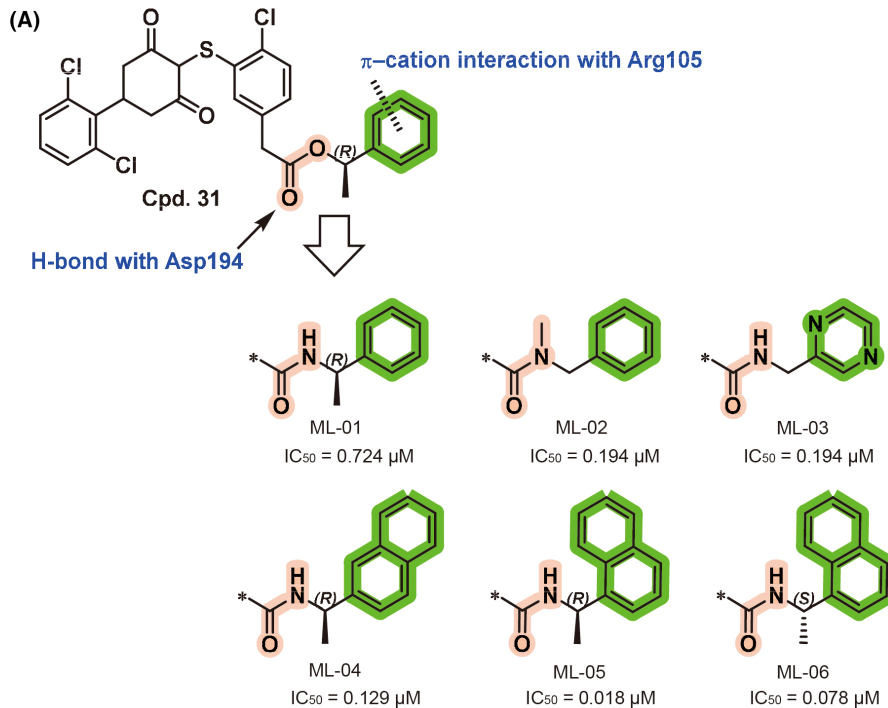
All data were expressed as mean \pm SEM, and unpaired Student's *t*-test, or one-way or two-way ANOVA followed by Tukey's multiple comparisons test as indicated. The statistical analyses were undertaken using GraphPad Prism (version 8.0.1) software. Other methods are shown in the Appendix S1.

3 | RESULTS

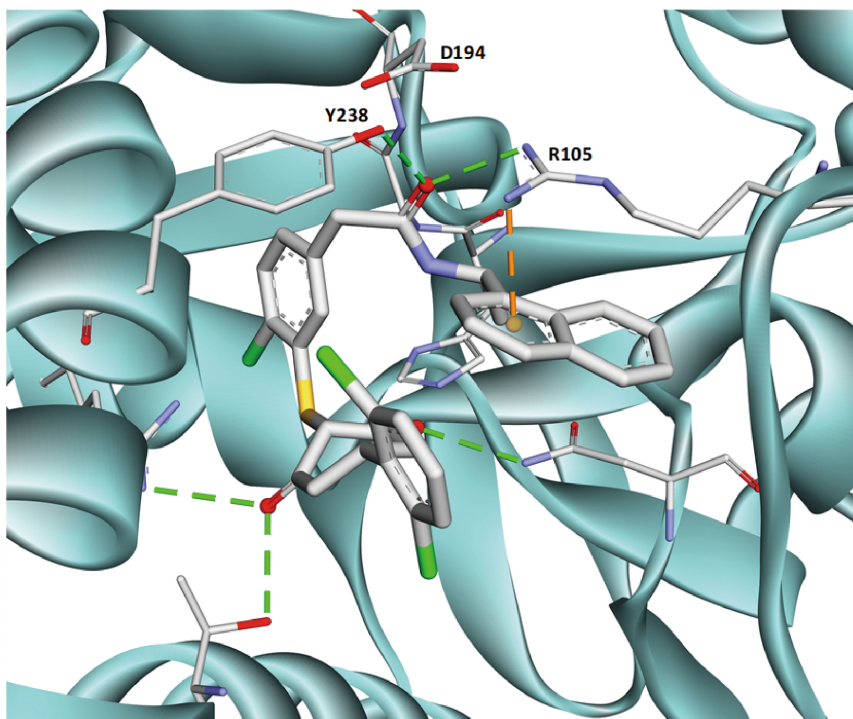
3.1 | Design of novel LDHA inhibitor ML-05

GNE140 is a potent LDHA inhibitor possessing good molecular (LDHA $\text{IC}_{50} = 3 \text{ nM}$) and cellular activity; however, it did not show antitumor activity in the MIA PaCa-2 xenograft model even at the dose of 400 mg/kg.²⁶ Genentech previously reported another series of diketone compounds as LDHA inhibitors.²⁴ Among them, compound 31 was optimized as the most potent analogue (LDHA $\text{IC}_{50} = 6 \text{ nM}$), however, this compound was found unstable in plasma due to its ester bond. To increase the in vivo stability, ML-01, an amide analogue of compound 31, was prepared and tested. However, it displayed a significant decrease of activity as compared to its parent compound 31 (Figure 2A). We envisioned that replacing the phenyl ring with various aromatic groups might increase the π -cation

FIGURE 2 Design of lactate dehydrogenase A (LDHA) inhibitors and molecule docking. (A) Structure-activity relationships of 3-hydroxy-2-mercaptocyclohex-2-enone-containing compounds. The biochemical IC_{50} for inhibition of LDHA for each compound is shown. (B) Docking studies on compound ML-05 with the crystal structure of LDHA protein (PDB code 4R68)



(B)



interaction with Arg105. A series of aromatic amides (ML-02–05) based on the 5-(2,6-dichlorophenyl)-3-hydroxy-2-mercaptocyclohex-2-enone scaffold were designed and synthesized (Figure 2A). From compounds ML-02 to ML-05, it was found that (*R*)-1-(1-naphthyl) ethylamine substitution (ML-05) displayed strong inhibitory activity against LDHA ($IC_{50} = 18 \text{ nM}$), replacement of naphthalene ring with pyrazine (ML-03) or 2-substituted naphthalene ring (ML-04) reduced the inhibitory activity by almost 7–10-fold, and *S*-enantiomer

of ML-05 (ML-06) reduced potency by almost 5-fold. To gain deep insight into the molecular basis on inhibitory activity, molecular docking of ML-05 was investigated by using Schrödinger. From the docking prediction, the naphthalene group enables favorable π -cation interaction with the guanidinium moiety of Arg105. In addition, the carbonyl of the amide moiety formed two hydrogen bonds, one with Tyr238 and one with Arg105 (Figure 2B), suggesting the importance of this functional group. We believe that these two

additional favorable interactions with the protein were responsible for the observed gain in potency for ML-05. As a result, compound ML-05 was selected for further evaluation.

3.2 | ML-05 inhibited lactate production and glycolysis in cultured cells

Human-derived cancer cells were used to test the inhibitory activity of ML-05 on lactate production. ML-05 dose-dependently inhibited the production of lactate in A375, CAL51, and MIA PACA2 cells with comparable potency with GNE140 after 6 h of treatment (Figure 3A–C). Furthermore, ML-05 was tested on the inhibition of lactate production in murine cancer cells. Similarly, ML-05 dose-dependently inhibited the lactate production in B16F10, EMT6, and Panc02 cells with comparable potency with GNE140 after 6 h of

treatment (Figure 3D–F). These data indicated that ML-05 could reduce lactate production in human-derived cells and murine-derived cells with comparable potency.

Melanoma is a highly glycolytic tumor, in which lactate induces an immunosuppressive TME and correlates with metastasis.^{28,29} Inhibition of LDHA activity exerts antitumor effects by promoting T cell infiltration.¹⁷ Thus, we selected melanoma cells (B16F10) for further evaluation of compound ML-05. To verify the inhibitory effect of ML-05 on glycolysis, a glycolytic stress test was carried out on B16F10 cells by transient injection of ML-05 or GNE140 and subsequently with glucose and oligomycin using Seahorse technology. The results showed that both ML-05 and GNE140 could dose-dependently inhibit ECAR and glycolysis capacity (Figure 3G–I), whereas ML-05 showed less reduction on ECAR compared to that of GNE140 (Figure 3H,I), suggesting the transient inhibition on lactate production is weaker for ML-05.

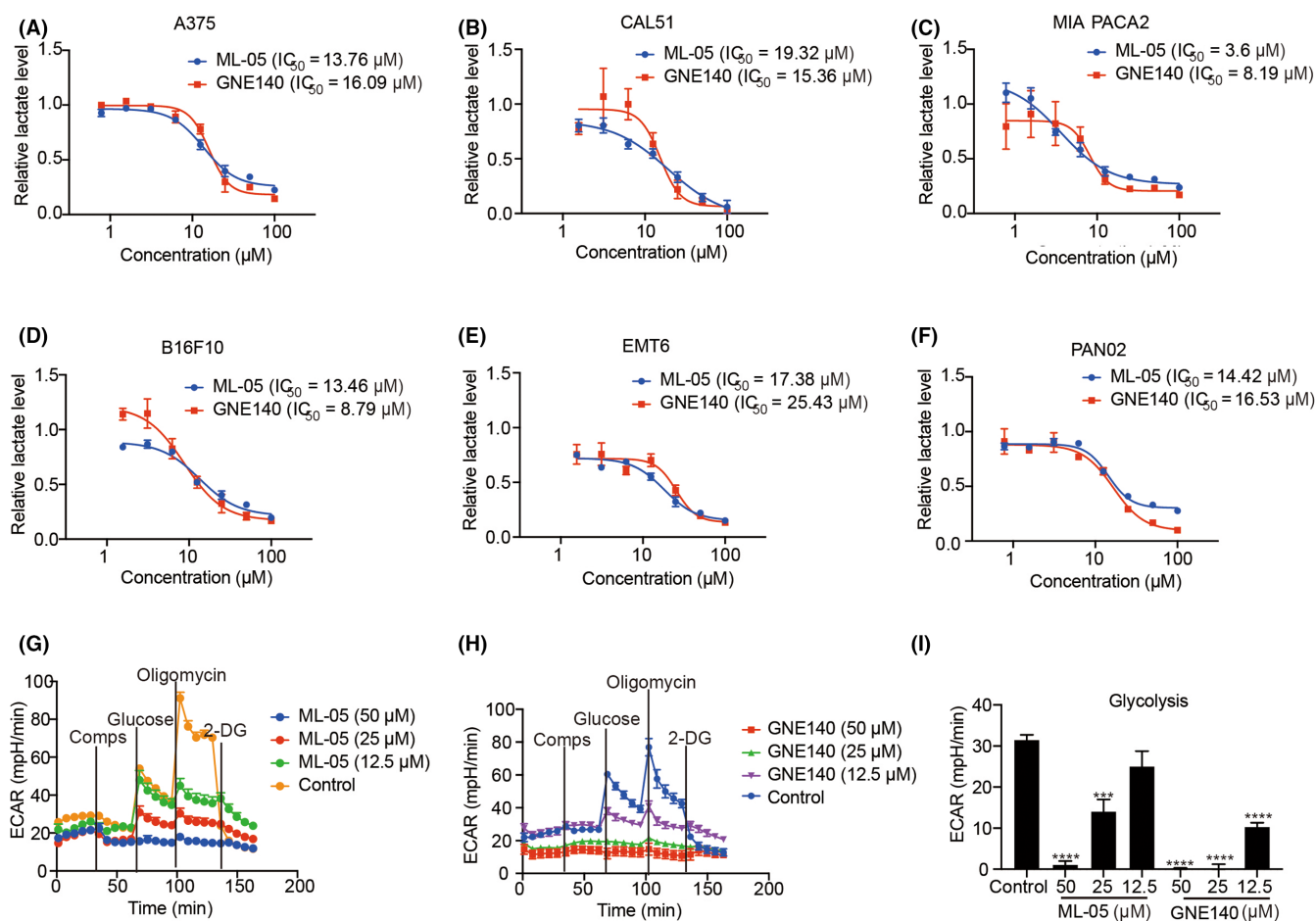


FIGURE 3 ML-05 inhibited lactate production and glycolysis in both human and murine cells. (A–C) Human cancer cells A375, CAL51, and MIA PACA2 were treated with serial doses of ML-05 or GNE140 for 6 h, and lactate levels in the supernatant were measured. Data are shown as mean \pm SEM, $n = 3$. (D–F) Murine cancer cells B16F10, EMT6, and Panc02 were treated with serial doses of ML-05 for 6 h, and lactate levels in the supernatant were measured. Data are shown as mean \pm SEM, $n = 3$. (G,H) Extracellular acidification rate (ECAR) curve of B16F10 cells as measured by Seahorse technology. Compounds (Comps) were injected as indicated, mean \pm SEM was plotted, $n = 5$. (I) ECAR of (G) and (H) after glucose injection, reflecting the glycolytic capacity. *** $p < 0.001$, **** $p < 0.0001$, compared to control group by using one-way ANOVA

3.3 | ML-05 inhibited cell proliferation and promoted ROS production and G₁ phase arrest

ML-05 has pan-inhibitory activity against human and murine cancer cells, with higher potency in A375, CAL51, MDA-MB-468, B16F10, 4T1, and PAN02 cells and less potency in MIA PACA-2, HMCB, EMT6, and LLC cells compared to GNE140 (Figure 4A). Specifically, the IC₅₀ of ML-05 on B16F10 cells was 23 μM and further explored for the mechanisms involved in the inhibition of cell proliferation. ML-05 dose-dependently inhibited ATP production of B16F10 cells (Figure 4B). Glycolysis reduces the carbon flow from pyruvate to the Krebs cycle, thus minimizing the production of ROS and allowing tumor cells to be protected from oxidative stress. Indeed, LDHA inhibition could promote ROS production, which induces oxidative stress and restrains tumor progression.¹⁹ Consistently, ML-05 promoted the production of ROS in B16F10 cells with the highest induction at 25 μM, while higher level of ML-05 (50 μM) induced less ROS might relate to the death of high ROS production cells (Figure 4C).

Next, we determined the effect of ML-05 on the cell cycle. ML-05 induced G₁ cell cycle arrest at all doses tested, and G₁ arrest was more pronounced at the two higher doses (25 and 50 μM) (Figure 4D,E). In addition, we examined the expression of c-Myc, p-Rb/Rb, CDK2, and cyclin A, which are G₁ cell cycle regulators. c-Myc and p-Rb/Rb are upstream positive regulators of the cell cycle, and we found their expression was reduced by ML-05 in a dose-dependent manner (Figure 4F). Concordantly, the association of cyclin A and CDK2 is required for G₁/S transition³¹ and thus their decrement by ML-05 treatment was associated with G₁ phase arrest. Collectively, these results indicated that ML-05 has a pan-inhibitory effect on cancer cell proliferation, which was associated with decrease in ATP production and increase in ROS production and G₁ phase arrest.

3.4 | ML-05 inhibited growth of B16F10 melanoma in immunocompetent mice

ML-05 did not inhibit the growth of B16F10 allograft tumor in immunocompetent C57BL/6 mice by oral administration or i.p. injection, similar to GNE140 (Figure S1A–D). Considering the intratumoral inhibition of lactate production might alleviate local immunosuppressive TME, we tested the antitumor effect of ML-05 by intratumoral injection. Interestingly, ML-05 could significantly inhibit the growth of B16F10 allograft tumor with a TGI rate of 60% and reduce the tumor weight, whereas GNE140 only showed modest antitumor activity without statistical difference on tumor growth or tumor weight (Figure 5A,B), and neither impacted on the body weight of mice (Figure 5C). The reduction of lactate production in tumor tissues was confirmed by measuring the lactate level after 6 h of ML-05 treatment before mice were killed (Figure S1E). To further confirm whether the antitumor effect of ML-05 is through the inhibition of LDHA activity, we used LDHA siRNA by intratumoral injection in the B16F10 allograft tumor model, to observe whether local knockdown of LDHA expression could exert antitumor effects. Consistently,

local knockdown of LDHA exerted significant tumor inhibition with a TGI rate of 40% (Figure 4D), which was less than the TGI rate of ML-05, suggesting that ML-05 inhibited the tumor growth mainly through the inhibition of LDHA.

We next asked whether the antitumor effect of ML-05 acted through the improvement of TME, as ML-05 was also able to directly inhibit cancer cell proliferation. Thus, we used nude mice implanted with B16F10 tumor cells, which are deficient in T cells. Interestingly, the antitumor effect of ML-05 was largely diminished in nude mice, and GNE140 also did not show significant inhibition of tumor growth or tumor weight in nude mice, nor on the body weight of mice (Figure 5E–G). These data suggested the antitumor effect of ML-05 acts mainly through immune activation, as direct tumor cell inhibition was insufficient to antagonize tumor growth. It should be noted that nude mice are deficient in T cells, suggesting that T cells might play an important role in the antitumor effect of ML-05.

3.5 | ML-05 increased Th1 and cytotoxic CD8T cells in TME

Given the antitumor effect of ML-05 was related to T cells and adaptive immunity, we further investigated how ML-05 impacts on tumor infiltrating immune cell subsets, which could account for the antitumor effect. The T cell subsets were gated, as shown in Figure 6A,B, and we found ML-05 treatment did not induce significant changes in CD3⁺ T, CD4⁺ T, or CD8⁺ T cells (Figure 6C–E). In a further analysis of the CD4⁺ T subsets, we found ML-05 but not GNE140 induced a significant increase in Th1 cells (Figure 6F), but neither had a significant influence on Th17 or Treg cells (Figure 6G,H). For the CD8⁺ T cell subsets, we found the levels of GMZB⁺CD8 T cells were dramatically increased by ML-05 but not GNE140 treatment (Figure 6I), with no significant change for IFN-γ⁺CD8⁺ T cells (Figure 6J). These results suggested the increase of Th1 and GMZB⁺CD8 T cells in the TME under ML-05 treatment could play a critical role in mediating its antitumor effect. In contrast, GNE140 did not show any impact on Th1 or GMZB⁺CD8 T cells in the TME, which could explain its marginal antitumor effect in vivo.

Furthermore, we also determined the changes in macrophages and subsets under ML-05 treatment, the functions of which are closely related to lactate level.^{31,32} However, the frequency of macrophages did not show significant changes after ML-05 treatment (Figure S2A), nor for the subsets, including M1 and M2 macrophages and M1 / M2 ratios (Figure S2B–D). These results suggested the frequency of tumor infiltrating macrophages were not significantly affected by ML-05. In addition, we further explored the influence of ML-05 on mouse primary macrophages, which were used to observe the effect of ML-05 on M1 and M2 differentiation under lactate co-incubation. We found that lactate co-incubation could decrease the differentiation of M1 and increase the differentiation of M2 from M0. ML-05 treatment significantly reversed the M1 and M2 macrophage differentiation (Figure S2E), suggesting that ML-05 could modulate the differentiation of macrophages under lactate induction.

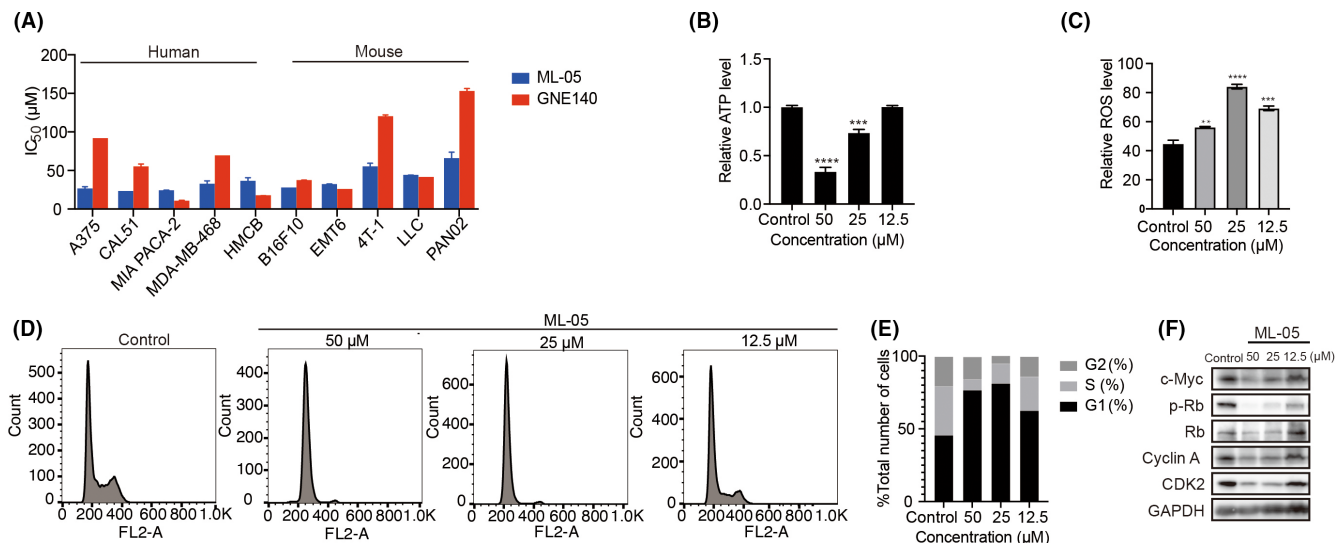


FIGURE 4 ML-05 inhibited cell proliferation and ATP production, and induced reactive oxygen species (ROS) production and G_1 phase arrest. (A) Antiproliferative activity of ML-05 or GNE140 against various human or murine cancer cell lines. Cancer cell lines were treated with serial concentrations of ML-05 or GNE140 for 72 h. IC_{50} (μ M) values are shown as mean \pm SEM from two or three independent experiments. (B) B16F10 cells were treated with ML-05 at indicated concentrations for 24 h. Cellular ATP levels were determined by fluorescence assay and normalized by the number of live cells, mean \pm SEM, $n = 3$. (C) B16F10 cells were treated with indicated concentrations of ML-05 for 24 h, and cellular ROS levels were determined by median DCFDA fluorescence. Mean \pm SEM, $n = 3$. (D) B16F10 cells were treated with indicated concentrations of ML-05 for 24 h, and the cell cycle was analyzed by propidium iodide staining. (E) Cell cycle distribution of (D). (F) B16F10 cells were treated with indicated concentrations of ML-05 for 24 h, and the expression of cell cycle associated proteins were measured by immunoblotting. ** $p < 0.01$, *** $p < 0.001$, **** $p < 0.0001$, compared to control group using one-way ANOVA

3.6 | ML-05 enhanced antitumor effects of PD-1 Ab and STING agonist

As ML-05 could increase Th1 and GMZB⁺ CD8T cells in B16F10 TME, we next determined whether it could enhance the efficacy of immunotherapy. Programmed cell death-1 is a well-known immune checkpoint, and PD-1 Ab has achieved great success in clinic patients bearing with “hot tumors”. However, a large proportion of “cold tumors” are refractory to anti-PD-1 therapy, and some studies have reported that the excessive lactate could induce an immunosuppressive TME.^{33,34} Therefore, we tested whether ML-05 and PD-1 Ab have a combined antitumor effect. In the B16F10 tumor model, PD-1 Ab was given i.p. twice a week, and ML-05 was given i.t. daily. As shown in Figure 7A, PD-1 Ab did not show significant inhibition of B16F10 tumor growth or weight, whereas the combination of ML-05 and PD-1 Ab exerted a much more dramatic inhibition on tumor growth and weight than monotherapy (Figure 7B), without impacting on body weight (Figure 7C).

Innate immunity is essential for immune surveillance and activating the innate immune signaling pathways is now emerging as an important strategy in cancer immunotherapy. Among them, STING agonist is a hot topic based on its potent activation on antitumor immune response. To explore the combined effect of ML-05 with STING agonist, we used a STING agonist (diABZI) developed by GSK.³⁵ In the B16F10 tumor model, diABZI was given i.p. and ML-05 was given i.t. We found a slightly higher inhibition of tumor growth in the combined group compared to monotherapy (Figure 7D). Tumor

weight was much lower in the combined treatment group compared monotherapy (Figure 7E), without impacting on body weight (Figure 7F).

4 | DISCUSSION

Glycolysis produces large amounts of lactic acid, which exacerbates the immunosuppressive TME and promotes tumor progression. Lactate dehydrogenase A is the main catalyzing enzyme for lactate production, and there were positive correlations between LDHA and tumor progression.^{36–38} Thus, inhibiting LDHA activity and lactate production is expected to promote the antitumor immune response or sensitize immunotherapy. GNE140 shows the most potent activity on LDHA inhibition, but did not show potent antitumor activity in vivo.²⁶ Similar to GNE140, ML-05 did not dramatically inhibit B16F10 tumor growth in vivo by systemic administration. Therefore, we hypothesized that targeting lactate production in local tumor tissue might be suitable to reverse the immunosuppressive TME. Intriguingly, this concept was confirmed by the intratumoral injection of ML-05, which showed a dramatic inhibition on B16F10 tumor growth in vivo. These results suggested that local treatment with an LDHA inhibitor could be an appropriate antitumor approach for future development.

Although we found the antiproliferative effect of ML-05 in cultured cancer cells, this effect was not sufficient to produce pronounced tumor inhibition in vivo, as shown in nude mice. Notably, the antitumor effect was observed in immunocompetent mice,

suggesting the restoration of immune response is critical to the anti-tumor effect of ML-05 *in vivo*. To explore the immune activation associated with ML-05 treatment, we analyzed the infiltrating immune cell subsets in B16F10 tumor tissues. Interestingly, we found that ML-05 treatment could dramatically increase the frequency of Th1 and GMZB⁺CD8 T cells, which are two important antitumor immune subsets.³⁹ In contrast, GNE140 did not show significant antitumor activity nor any effect on T cell infiltration in tumors, which might relate to its metabolic or other issues; the exact mechanism needs to be further explored. Notably, highly glycolytic tumors could dampen T cell antitumor activity by limiting glucose use and promoting lactate accumulation.^{9,17,40,41,42} Lactate dehydrogenase A could affect the immune response of T cells through the PI3K-Akt-Foxo1 pathway,⁴³ and high lactate levels inhibited cytokine production and impaired the lytic function of cytotoxic T cells.⁴⁴ Our results substantiated that the inhibition of LDHA could restore the antitumor immunity of Th1 and GMZB⁺ CD8 T cells in melanoma, although it did not have a significant impact on total T cells, CD4⁺ T cells, or CD8⁺ T

cells. Lactate could polarize macrophages to an M2-like state but inhibit the polarization to an M1-like state that favors tumor growth.⁴⁵ However, there were no significant changes in the frequencies of M1-like or M2-like macrophages, which might relate to their dynamic changes in the TME under ML-05 treatment; however, we might not have captured the changes in macrophages at the right time. Thus, we tested the influence of ML-05 on macrophages in primary macrophages, and found that ML-05 could reverse the polarization of M2 and M1 induced by lactate. Therefore, the reactivation of macrophage function by ML-05 might also contribute to antitumor activity, which could further promote the activation of Th1 and GMZB⁺ CD8 T cells. Given the complex and dynamic changes of immune subsets in the TME under ML-05 treatment, further study is required to fully determine the impact of ML-05 on immune activation.

Furthermore, we asked whether LDHA inhibitor could sensitize immunotherapy. As is well-known, B16F10 is a “cold tumor” that is resistant to PD-1/L1 therapy, thus we tested whether ML-05 could sensitize the antitumor effect of PD-1 Ab in the B16F10 tumor

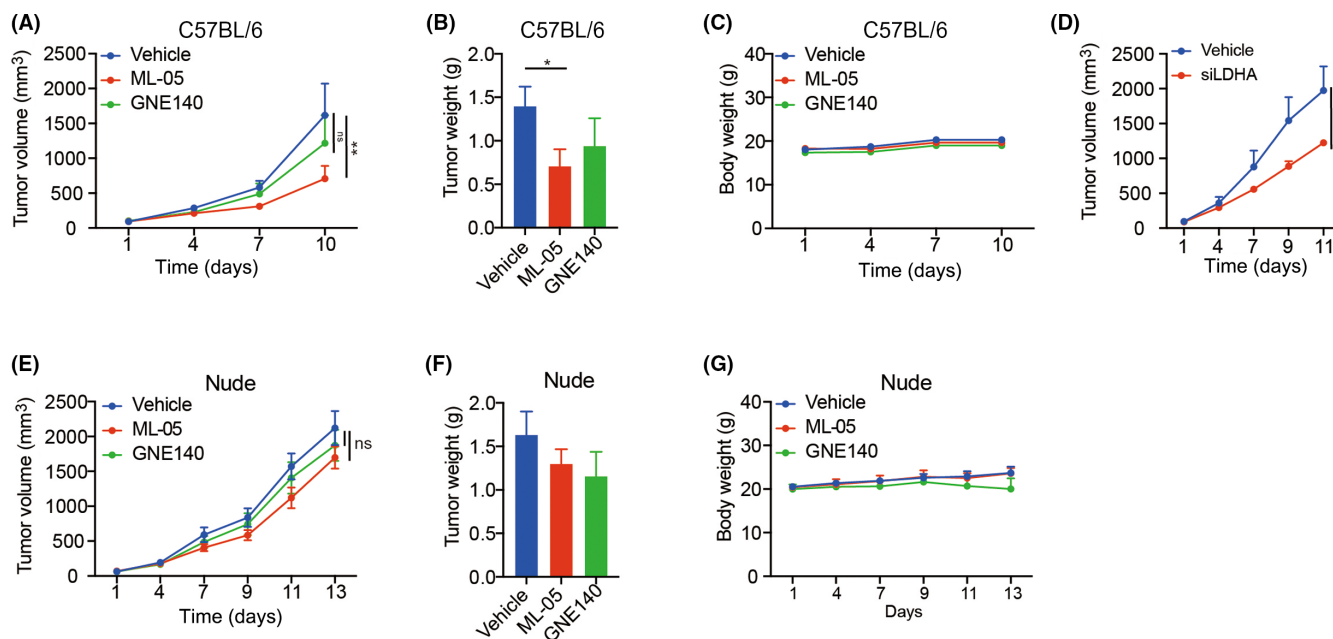
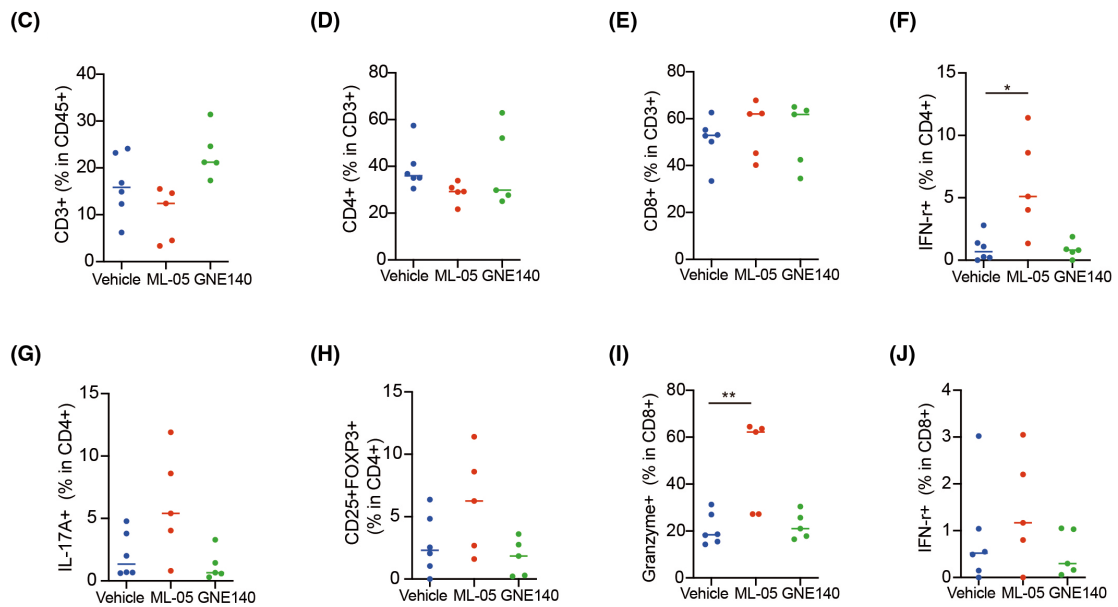
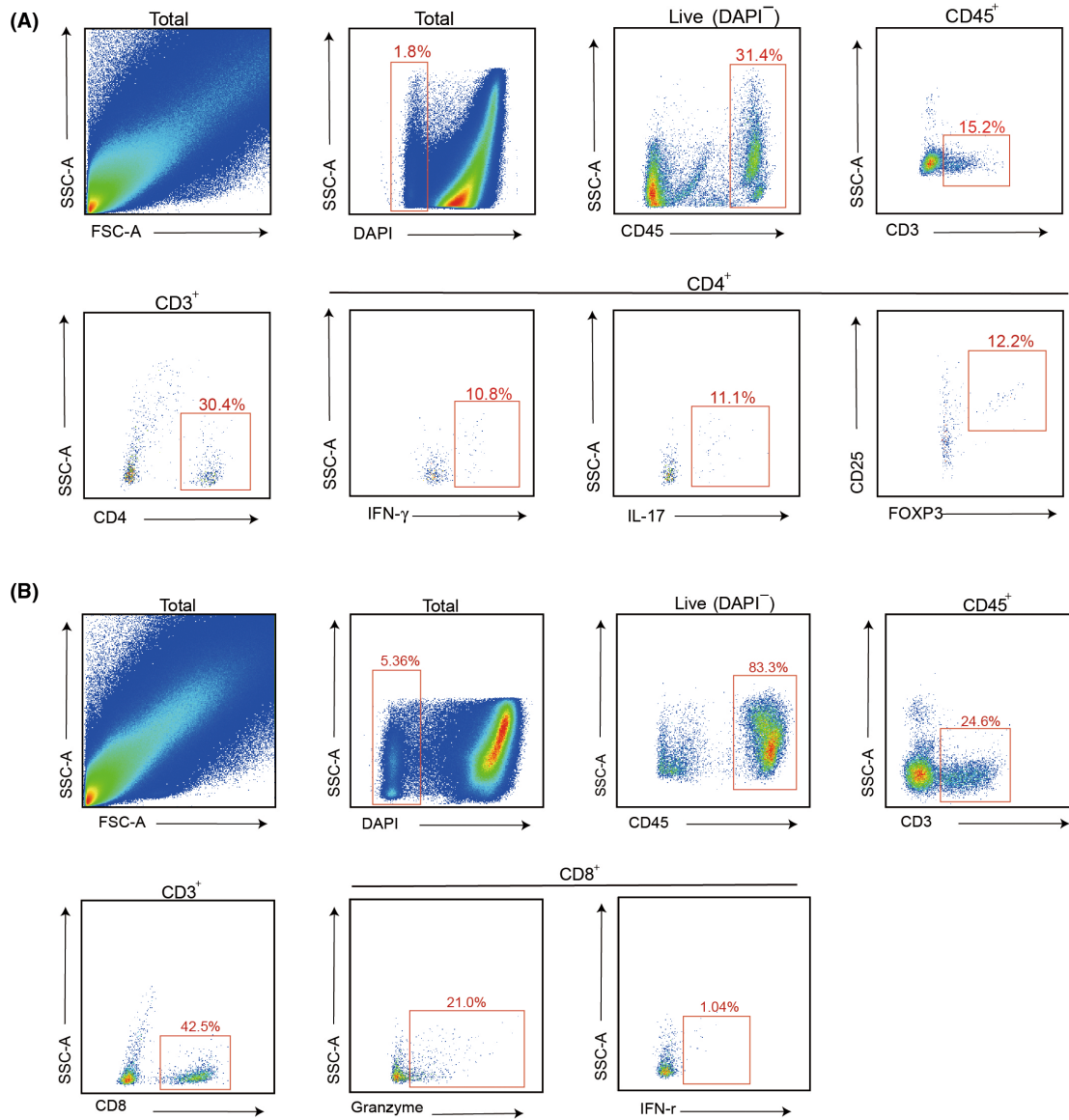


FIGURE 5 In vivo antitumor effect of ML-05. (A) Effect of ML-05 on B16F10 tumor growth in C57BL/6 mice. Tumors were intratumorally injected with vehicle (5% DMSO +5% Kolliphor HS15), ML-05 (50mg/kg), or GNE140 (50mg/kg) per day. Data represent mean \pm SEM, $n = 6$. *** $p < 0.001$, two-way ANOVA. ns, no statistical significance. (B) Tumor weight. * $p < 0.05$, one-way ANOVA. (C) Body weight of mice shown in (A). (D) Effect of lactate dehydrogenase A (LDHA) siRNA treatment on B16F10 tumor growth in C57BL/6 mice. siLDHA (5 mmol) was intratumorally injected twice a week. Results represent mean \pm SEM, $n = 6$. * $p < 0.05$, two-way ANOVA. (E) Effect of ML-05 or GNE140 on B16F10 tumor growth in nude mice. Tumors were intratumorally injected with vehicle or ML-05 or GNE140 (50mg/kg) per day. Data represent mean \pm SEM, $n = 6$, two-way ANOVA. ns, no significant difference. (F) Tumor weight. (G) Body weight of mice of (E)

FIGURE 6 Effect of lactate dehydrogenase A (LDHA) inhibition on infiltrating immune cells in B16F10 tumors. B16F10 tumors were intratumorally treated with vehicle, ML-05, or GNE140 (50mg/kg/day), and tumor infiltrating immune cells were determined by flow cytometry. (A,B) Gating strategy for the CD4⁺ T subsets and CD8⁺ T subsets of flow cytometry analysis. Numbers in graphs indicate the percentage of cells. Plots of data from representative ML-05 samples are shown. (C) CD3⁺ T cells. (D) CD4⁺ T cells. (E) CD8⁺ T cells. (F) Interferon- γ (IFN- γ)⁺CD4⁺ T cells (T helper 1). (G) Interleukin (IL)-17A⁺CD4⁺ T cells (Th17). (H) CD25⁺ and FOXP3⁺ CD4⁺ T cells (regulatory T cells). (I) Granzyme B⁺CD8⁺ T cells. (J) IFN- γ ⁺CD8⁺ T cells. Data are represented as mean \pm SEM, $n = 5-6$. Plot data from representative tumors are shown. * $p < 0.05$, ** $p < 0.01$, one-way ANOVA. FSC, forward scatter; ns, no statistical significance; SSC, side scatter



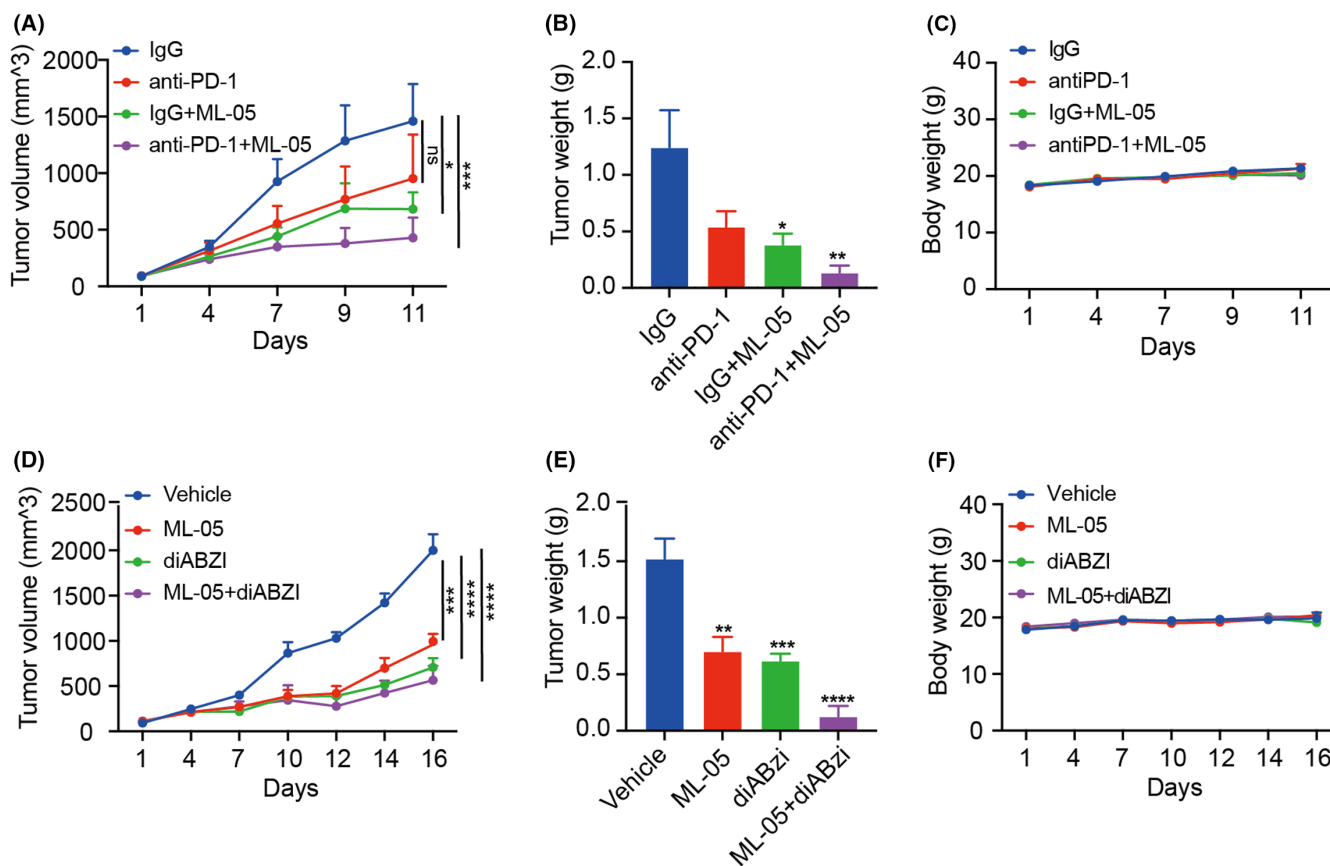


FIGURE 7 Combined antitumor effect of ML-05 with programmed cell death-1 (PD-1) Ab or stimulator of interferon genes (STING) agonist. (A–C) B16F10 tumor model in C57 mice was treated with ML-05 (50 mg/kg/day) and PD-1 Ab (10 mg/kg, twice a week) alone or in combination. (D,E) B16F10 tumor model in C57 mice was treated with ML-05 (50 mg/kg/day) and diamidobenzimidazole (diABZI; 0.5 mg/kg, day 1, 4, 7) alone or in combination. Tumor volume was measured every 3 days, and the tumor growth was compared by two-way ANOVA. Tumor weight was compared with vehicle group by one-way ANOVA. * $p < 0.05$, ** $p < 0.01$, *** $p < 0.001$. **** $p < 0.0001$ compared to vehicle group

model. Interestingly, the combined use of ML-05 and PD-1 Ab produced much higher inhibition of B16F10 tumor growth, suggesting the ML-05 could turn “cold tumors” to “hot tumors” and has the potential to expand the patient population that benefits from immune checkpoint therapy. This finding is concordant with the knockout of LDHA in mice with enhanced response to CTLA-4 Ab.⁴⁷ In addition, activating the innate immunity is emerging as a novel antitumor strategy; among them, STING stands out as a promising new target.^{48–50} Herein, we tested the combination of ML-05 with a STING agonist, diABZI. Although there was only a slight increase in the inhibition of tumor growth compared to monotherapy, the tumor weight of the combined group decreased remarkably, suggesting the tumor tissues became more “inflamed” with combined therapy. These results indicated the LDHA inhibitor could sensitize both innate and adaptive immunotherapy.

In summary, we developed a novel LDHA inhibitor, ML-05, which showed potent inhibition on lactate production, ROS production, and cell cycle arrest. ML-05 could release antitumor immunity through increasing the function of Th1 and GMZB⁺ CD8⁺ T cells in

vivo and potentially macrophages, suggesting it has the potential to turn “cold tumors” into “hot tumors”. Importantly, inhibition of LDHA in the local TME could sensitize immunotherapies, like PD-1 Ab and STING agonist, which might expand the number of patients that would benefit from their clinical application; inhibition of LDHA demonstrated great translational value. These findings underscore that targeting LDHA in the local TME is a feasible antitumor strategy, especially for glycolytic-dependent tumors, and provide a basis for development of LDHA inhibitors in the future.

ACKNOWLEDGMENTS

The authors gratefully acknowledge the financial support by the National Natural Science Foundation of China for Innovation Research Group (81821005), Shanghai Pujiang Program (18PJD052), and the Collaborative Innovation Cluster Project of Shanghai Municipal Commission of Health and Family Planning (2020CXJQ02).

DISCLOSURE

The authors declare no conflicts of interest.

ETHICS STATEMENT

Approval of the research protocol by an Institutional Review Board: N/A.

Informed consent: N/A.

Registry and registration no. of the study/trial: N/A.

Animal studies: Approved by the Animal Care and Use Committee of the Shanghai Institute of Materia Medica and performed according to the Ethics Guidelines for Animal Care.

ORCID

Zuoquan Xie  <https://orcid.org/0000-0002-1613-3321>

REFERENCES

1. Buck MD, Sowell RT, Kaech SM, Pearce EL. Metabolic instruction of immunity. *Cell*. 2017;169(4):570-586.
2. Sun L, Suo C, Li S-T, Zhang H, Gao P. Metabolic reprogramming for cancer cells and their microenvironment: beyond the Warburg effect. *Biochim Biophys Acta Rev Cancer*. 2018;1870(1):51-66.
3. Leone RD, Powell JD. Metabolism of immune cells in cancer. *Nat Rev Cancer*. 2020;20(9):516-531.
4. Hirschhaeuser F, Sattler UG, Mueller-Klieser W. Lactate: a metabolic key player in cancer. *Cancer Res*. 2011;71(22):6921-6925.
5. Gottfried E, Kunz-Schughart LA, Ebner S, et al. Tumor-derived lactic acid modulates dendritic cell activation and antigen expression. *Blood*. 2006;107(5):2013-2021.
6. Li W, Tanikawa T, Kryczek I, et al. Aerobic glycolysis controls myeloid-derived suppressor cells and tumor immunity via a specific cebpb isoform in triple-negative breast cancer. *Cell Metab*. 2018;28(1):87-103.e6.
7. Yang X, Lu Y, Hang J, et al. Lactate-modulated immunosuppression of myeloid-derived suppressor cells contributes to the radioresistance of pancreatic cancer. *Cancer Immunol Res*. 2020;8(11):1440-1451.
8. Brand A, Singer K, Koehl GE, et al. LDHA-associated lactic acid production blunts tumor immunosurveillance by T and NK cells. *Cell Metab*. 2016;24(5):657-671.
9. Zhang L, Romero P. Metabolic control of CD8⁺ T cell fate decisions and antitumor immunity. *Trends Mol Med*. 2018;24(1):30-48.
10. Rabinowitz JD, Enerbäck S. Lactate: the ugly duckling of energy metabolism. *Nat Metab*. 2020;2(7):566-571.
11. Koukourakis MI, Giatromanolaki A, Winter S, Leek R, Sivridis E, Harris AL. Lactate dehydrogenase 5 expression in squamous cell head and neck cancer relates to prognosis following radical or post-operative radiotherapy. *Oncology*. 2009;77(5):285-292.
12. Mishra D, Banerjee D. Lactate dehydrogenases as metabolic links between tumor and stroma in the tumor microenvironment. *Cancers (Basel)*. 2019;11(6):750.
13. Wang ZY, Loo TY, Shen JG, et al. LDH-A silencing suppresses breast cancer tumorigenicity through induction of oxidative stress mediated mitochondrial pathway apoptosis. *Breast Cancer Res Treat*. 2012;131(3):791-800.
14. Fantin VR, St-Pierre J, Leder P. Attenuation of LDH-A expression uncovers a link between glycolysis, mitochondrial physiology, and tumor maintenance. *Cancer Cell*. 2006;9(6):425-434.
15. Xie H, Hanai JI, Ren JG, et al. Targeting lactate dehydrogenase-A inhibits tumorigenesis and tumor progression in mouse models of lung cancer and impacts tumor-initiating cells. *Cell Metab*. 2014;19(5):795-809.
16. Seth P, Csizmadia E, Hedblom A, et al. Deletion of lactate dehydrogenase-A in myeloid cells triggers antitumor immunity. *Cancer Res*. 2017;77(13):3632-3643.
17. Cascone T, McKenzie JA, Mbofung RM, et al. Increased tumor glycolysis characterizes immune resistance to adoptive T cell therapy. *Cell Metab*. 2018;27(5):977-987.e4.
18. Busch H, Nair PV. Inhibition of lactic acid dehydrogenase by fluoropyruvic acid. *J Biol Chem*. 1957;229(1):377-387.
19. Le A, Cooper CR, Gouw AM, et al. Inhibition of lactate dehydrogenase A induces oxidative stress and inhibits tumor progression. *Proc Natl Acad Sci USA*. 2010;107(5):2037-2042.
20. Granchi C, Roy S, De Simone A, et al. N-Hydroxyindole-based inhibitors of lactate dehydrogenase against cancer cell proliferation. *Eur J Med Chem*. 2011;46(11):5398-5407.
21. Ward RA, Brassington C, Breeze AL, et al. Design and synthesis of novel lactate dehydrogenase inhibitors by fragment-based lead generation. *J Med Chem*. 2012;55(7):3285-3306.
22. Dragovich PS, Fauber BP, Corson LB, et al. Identification of substituted 2-thio-6-oxo-1,6-dihydropyrimidines as inhibitors of human lactate dehydrogenase. *Bioorganic Med Chem Lett*. 2013;23(11):3186-3194.
23. Fauber BP, Dragovich PS, Chen J, et al. Identification of 2-amino-5-aryl-pyrazines as inhibitors of human lactate dehydrogenase. *Bioorganic Med Chem Lett*. 2013;23(20):5533-5539.
24. Dragovich PS, Fauber BP, Boggs J, et al. Identification of substituted 3-hydroxy-2-mercaptocyclohex-2-enones as potent inhibitors of human lactate dehydrogenase. *Bioorganic Med Chem Lett*. 2014;24(16):3764-3771.
25. Billiard J, Dennison JB, Briand J, et al. Quinoline 3-sulfonamides inhibit lactate dehydrogenase A and reverse aerobic glycolysis in cancer cells. *Cancer Metab*. 2013;1(1):1-17.
26. Boudreau A, Purkey HE, Hitz A, et al. Metabolic plasticity underpins innate and acquired resistance to LDHA inhibition. *Nat Chem Biol*. 2016;12(10):779-786.
27. Rai G, Brimacombe KR, Mott BT, et al. Discovery and optimization of potent, cell-active pyrazole-based inhibitors of lactate dehydrogenase (LDH). *J Med Chem*. 2017;60(22):9184-9204.
28. Labadie S, Dragovich PS, Chen J, et al. Optimization of 5-(2,6-dichlorophenyl)-3-hydroxy-2-mercaptocyclohex-2-enones as potent inhibitors of human lactate dehydrogenase. *Bioorganic Med Chem Lett*. 2015;25(1):75-82.
29. Piskounova E, Agathocleous M, Murphy MM, et al. Oxidative stress inhibits distant metastasis by human melanoma cells. *Nature*. 2015;527(7577):186-191.
30. Bohn T, Rapp S, Luther N, et al. Tumor immunoevasion via acidosis-dependent induction of regulatory tumor-associated macrophages. *Nat Immunol*. 2018;19(12):1319-1329.
31. Pietenpol JA, Stewart ZA. Cell cycle checkpoint signaling: cell cycle arrest versus apoptosis. *Toxicology*. 2002;181-182:475-481.
32. Vitale I, Manic G, Coussens LM, Kroemer G, Galluzzi L. Macrophages and metabolism in the tumor microenvironment. *Cell Metab*. 2019;30(1):36-50.
33. Ke X, Chen C, Song Y, et al. Hypoxia modifies the polarization of macrophages and their inflammatory microenvironment, and inhibits malignant behavior in cancer cells. *Oncol Lett*. 2019;18(6):5871-5878.
34. Noman MZ, Desantis G, Janji B, et al. PD-L1 is a novel direct target of HIF-1 α , and its blockade under hypoxia enhanced: MDSC-mediated T cell activation. *J Exp Med*. 2014;211(5):781-790.
35. Li X, Wenes M, Romero P, Huang SCC, Fendt SM, Ho PC. Navigating metabolic pathways to enhance antitumor immunity and immunotherapy. *Nat Rev Clin Oncol*. 2019;16(7):425-441.
36. Ramanjulu JM, Pesiridis GS, Yang J, et al. Design of amidobenzimidazole STING receptor agonists with systemic activity. *Nature*. 2018;564(7736):439-443.
37. Zhuang L, Scolyer RA, Murali R, et al. Lactate dehydrogenase 5 expression in melanoma increases with disease progression and is

- associated with expression of Bcl-XL and Mcl-1, but not Bcl-2 proteins. *Mod Pathol.* 2010;23(1):45-53.
38. Hermes A, Gatzemeier U, Waschki B, Reck M. Lactate dehydrogenase as prognostic factor in limited and extensive disease stage small cell lung cancer - a retrospective single institution analysis. *Respir Med.* 2010;104(12):1937-1942.
 39. Kayser G, Kassem A, Sienel W, et al. Lactate-dehydrogenase 5 is overexpressed in non-small cell lung cancer and correlates with the expression of the transketolase-like protein 1. *Diagn Pathol.* 2010;5(1):1-10.
 40. Schreiber RD, Old LJ, Smyth MJ. Cancer immunoediting: integrating immunity's roles in cancer suppression and promotion. *Science (80-).* 2011;331(6024):1565-1570.
 41. Haas R, Smith J, Rocher-Ros V, et al. Lactate regulates metabolic and proinflammatory circuits in control of T cell migration and effector functions. *PLoS Biol.* 2015;13(7):1-24.
 42. Cham CM, Driessens G, O'Keefe JP, Gajewski TF. Glucose deprivation inhibits multiple key gene expression events and effector functions in CD8⁺ T cells. *Eur J Immunol.* 2008;38(9):2438-2450.
 43. Macintyre AN, Gerriets VA, Nichols AG, et al. The glucose transporter Glut1 is selectively essential for CD4 T cell activation and effector function. *Cell Metab.* 2014;20(1):61-72.
 44. Xu K, Yin N, Peng M, et al. Glycolysis fuels phosphoinositide 3-kinase signaling to bolster T cell immunity. *Science (80-).* 2021;371(6527):405-410.
 45. Mendler AN, Hu B, Prinz PU, Kreutz M, Gottfried E, Noessner E. Tumor lactic acidosis suppresses CTL function by inhibition of p38 and JNK/c-Jun activation. *Int J Cancer.* 2012;131(3):633-640.
 46. Russell DG, Huang L, BC VV. Immunometabolism at the interface between macrophages and pathogens. *Nat Rev Immunol.* 2019;19(5):291-304.
 47. Zappasodi R, Serganova I, Cohen IJ, et al. HHS Public Access. 2021;591(7851):652-658.
 48. Woo SR, Fuertes MB, Corrales L, et al. STING-dependent cytosolic DNA sensing mediates innate immune recognition of immunogenic tumors. *Immunity.* 2014;41(5):830-842.
 49. Barber GN. STING: infection, inflammation and cancer. *Nat Rev Immunol.* 2015;15(12):760-770.
 50. Fuertes MB, Woo SR, Burnett B, Fu YX, Gajewski TF. Type I interferon response and innate immune sensing of cancer. *Trends Immunol.* 2013;34(2):67-73.

SUPPORTING INFORMATION

Additional supporting information can be found online in the Supporting Information section at the end of this article.

How to cite this article: Du M, Yu T, Zhan Q, et al. Development of a novel lactate dehydrogenase A inhibitor with potent antitumor activity and immune activation. *Cancer Sci.* 2022;113:2974-2985. doi: [10.1111/cas.15468](https://doi.org/10.1111/cas.15468)